Article

Cell Reports

The Ventral Hippocampus Controls Stress-Provoked Impulsive Aggression through the Ventromedial Hypothalamus in Post-Weaning Social Isolation Mice

Graphical Abstract

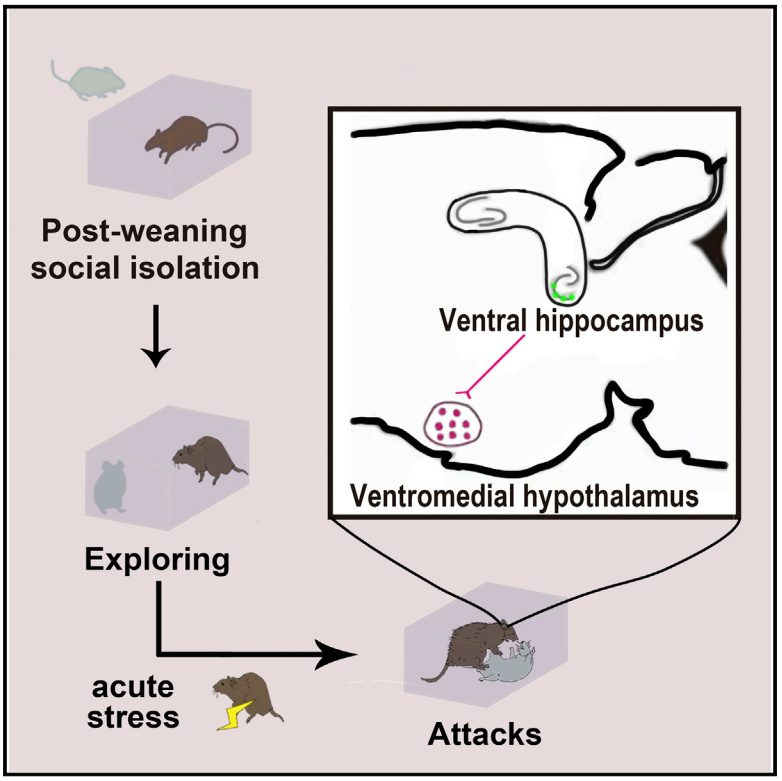

Authors

Chih-Hua Chang, Po-Wu Gean

Correspondence

powu@mail.ncku.edu.tw

In Brief

Individuals with a tendency toward impulsive aggression may suddenly attack others when under stress. The neural circuitry underlying stress-provoked aggression is largely unknown. Chang and Gean demonstrate that ventral hippocampal (vHip) outputs to the ventromedial hypothalamus (VMH) mediate stress-provoked aggression in post-weaning socially isolated mice.

Highlights

- Acute stress elicits attack behavior in the post-weaning socially isolated mice
- Activation of ventral hippocampal (vHip) neurons induces this attack behavior
- Inhibition of vHip neurons blocks stress-induced attack behavior
- vHip outputs to the ventromedial hypothalamus modulate attack behavior

Chang & Gean, 2019, Cell Reports *28*, 1195–1205
July 30, 2019
https://doi.org/10.1016/j.celrep.2019.07.005

CellPress

Cell Reports
Article

The Ventral Hippocampus Controls Stress-Provoked Impulsive Aggression through the Ventromedial Hypothalamus in Post-Weaning Social Isolation Mice

Chih-Hua Chang[1] and Po-Wu Gean[1,2,3,*]
[1]Department of Pharmacology, National Cheng-Kung University, Tainan 701, Taiwan
[2]Department of Biotechnology and Bioindustry Sciences, National Cheng-Kung University, Tainan 701, Taiwan
[3]Lead Contact
*Correspondence: powu@mail.ncku.edu.tw
https://doi.org/10.1016/j.celrep.2019.07.005

SUMMARY

Impulsively aggressive individuals may suddenly attack others when under stress, but the neural circuitry underlying stress-provoked aggression is poorly understood. Here, we report that acute stress activates ventral hippocampus (vHip) neurons to induce attack behavior in post-weaning socially isolated mice. Chemogenetic inhibition of vHip neural activity blunts stress-provoked attack behavior, whereas chemogenetic activation promotes it. The activation of cell bodies in vHip neurons projecting into the ventromedial hypothalamus (VMH) induces attack behavior, suggesting that the vHip-VMH projection contributes to impulsive aggression. Furthermore, optogenetic inhibition of vHip glutamatergic neurons blocks stress-provoked attacks, whereas optogenetic activation of vHip glutamatergic neurons drives attack behavior. These results show direct evidence that vHip-VMH neural circuitry modulates attack behavior in socially isolated mice.

INTRODUCTION

Aggression is an innate behavior in most animal species and can be useful for obtaining food, protecting territory, and maintaining mating rights. However, an inability to control aggression brings enormous problems to human society. Pathological aggression is attack behavior that occurs out of context, is out of proportion to the triggering cause, and/or is focused toward the vulnerable parts of the intruder (Miczek et al., 2013). For example, subjects with psychiatric illnesses, such as antisocial personality disorders, borderline personality disorders, bipolar disorders, and dementia, have a tendency to resort to out of control aggression when under acute stress (Dorfman et al., 2014).

The ventromedial hypothalamus (VMH) is a well-studied area of the brain that has been implicated in triggering attack behavior in mice. Previous studies have established a direct causal relationship between the VMH and aggression through genetic, optogenetic, and chemogenetic approaches. The activation of VMH neurons triggers immediate and direct attack behavior (Lee et al., 2014; Lin et al., 2011; Yang et al., 2017). However, it is still unclear how neural networks modulate the VMH to control aggression during various emotional and physiological states and in response to different environmental factors.

The brain areas known as the hippocampus is heterogeneous along its longitudinal axis. Although the dorsal region is involved in spatial memory, the ventral hippocampus (vHip) regulates emotions, motivation, and defensive behaviors, which often improve organisms' chance of survival when faced with life-threatening dangers (Maggio and Segal, 2012). The vHip has strong connections with the medial prefrontal cortex (mPFC), lateral septum (LS), the bed nucleus of stria terminalis (BNST), the medial amygdala (MeA), and the hypothalamus (Sahay and Hen, 2007). These vHip-connecting brain areas also are involved in the regulation of aggression (Anderson, 2012; Leroy et al., 2018; Takahashi et al., 2014; Toth et al., 2010; Unger et al., 2015; Wong et al., 2016). The vHip output, in particular, has been shown to project into the VMH (Chiba, 2000; Strange et al., 2014). Interestingly, the repeated electrical stimulation that evokes afterdischarges but not motor seizures (partial kindling) in the vHip has been reported to mediate aggression in cats, perhaps through the amygdalo-VMH pathway (Adamec, 1991; Adamec and Stark-Adamec, 1983). These studies suggest that vHip projections may be involved in the modulation of aggression.

The post-weaning social isolation (SI) is well-established as a useful animal model to study aggression. In rats, the SI rats attack vulnerable parts of those perceived as a danger (Toth et al., 2011). Similarly, SI mice exhibit a deficient prepulse inhibition of the acoustic startle reflex, depression-like behavior, and an increase in intimidating behavior, such as aggressive grooming and tail rattling (Chang et al., 2015). Moreover, acute stress induces outbursts of attack behavior in SI mice, although not in group-housed (GH) mice (Chang et al., 2015; Chang et al., 2018), which is similar to the reactive-impulsive aggression in subjects with psychiatric illnesses. It is reported that subjects with borderline personality disorders, whose core symptoms include trait aggression and impulsivity, have higher activation (Radaelli et al., 2012) and volume reduction (Rossi et al., 2012; Ruocco et al., 2012) in the anterior hippocampus (referred to as the vHip in mice). Similarly, the SI mice have hyper-activation of the vHip and overexpression of the NR2B subunit of N-methyl-D-aspartate (NMDA) receptors in the vHip. The

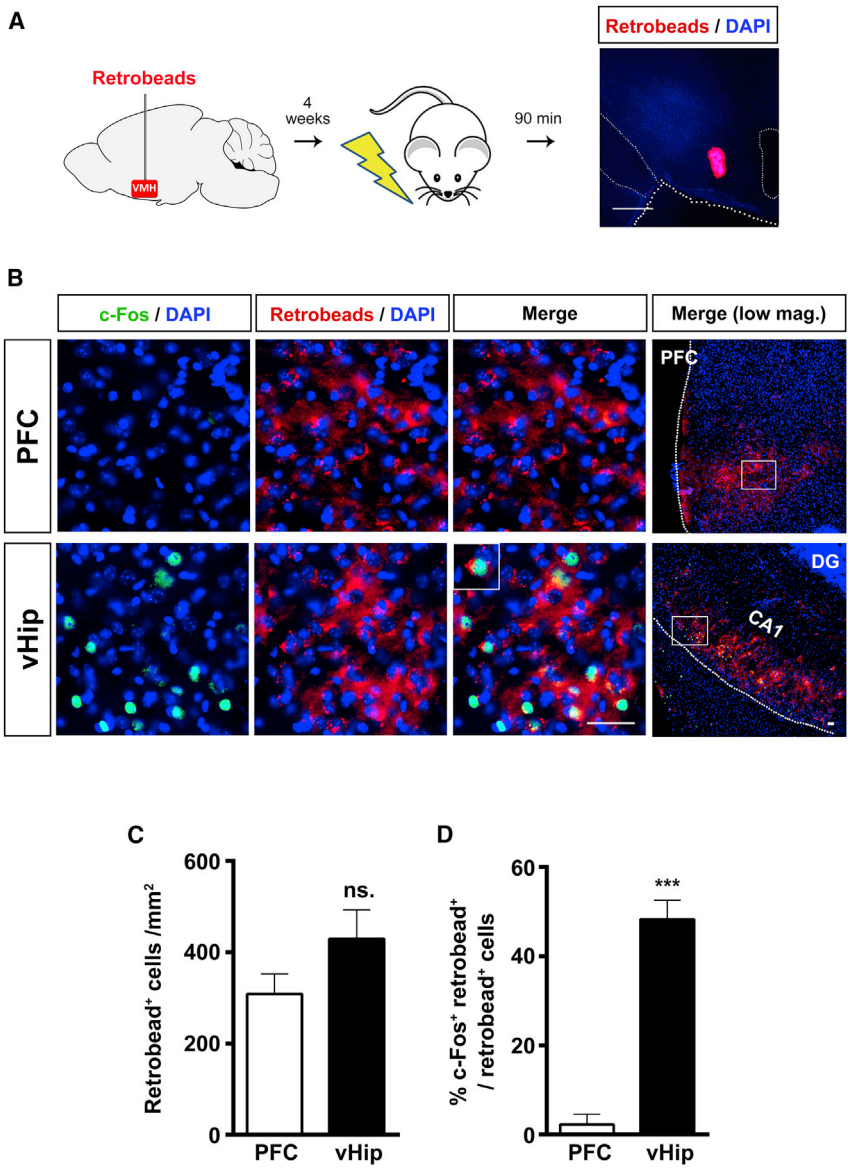

Figure 1. Acute Stress Activates vHip Neurons Projecting into the VMH

(A) Schematic representation of the experimental procedure and an image showing the red retrobead injection site in the VMH. Scale bar represents 550 μm.

(B) Representative images showing c-Fos- (green) and red retrobead-positive neurons as well as double-labeled neurons in the PFC (top) and the vHip (bottom). Scale bar represents 20 μm; inset, 1.3× magnification of the merged image; n = 3 mice.

(C) Cell number of red retrobead-positive neurons in the vHip and PFC.

(D) The c-Fos was selectively expressed in retrobead-positive neurons in the vHip but not in retrobead-positive neurons in the PFC (unpaired t test, $t = 9.46$, ***$p < 0.001$).

Data are represented as mean ± SEM.

blockade of NMDA receptors, especially NR2B, blocks stress-induced outbursts of attack behavior in SI mice (Chang et al., 2015). These studies indicate that subjects with a high tendency of reactive aggression exhibit impaired vHip functions. Although the blockade of NMDA receptors in the vHip inhibits attack behavior (Chang et al., 2015; Chang et al., 2018), there is so far no direct evidence to prove the vHip mediates aggression. To test this, in the present research we used red retrobeads to trace the vHip projection and manipulate vHip activity using designer receptors exclusively activated by designer drugs (DREADDs) and optogenetic approaches to examine the attack behavior of SI mice. We find that acute stress activates the vHip neurons projecting into the VMH (as the VMH-projecting vHip neurons). Moreover, the chemogenetic and optogenetic inhibition of the vHip activity decreases stress-induced outbursts of attack behavior. In contrast, chemogenetic and optogenetic activation of the vHip induces attack behavior. Furthermore, chemogenetic inhibition of the vHip terminals in the VMH suppresses attack behavior, whereas chemogenetic stimulation of vHip neurons projecting into the VMH induces attack behavior. Thus, the present study shows direct evidence that the function of the vHip-VMH neural pathway is to modulate stress-provoked attack behavior in mice.

RESULTS

Acute Stress Induces Neuronal Activation in the vHip that Is Projected into the VMH

The VMH, particularly the ventrolateral part of the VMH, is a well-studied brain region that can be induced to initiate aggressive behaviors through electric or optogenetic stimulation (Hashikawa et al., 2017; Lin et al., 2011). Conversely, the inhibition of neural activity in this area blocks natural inter-male attack behavior (Lin et al., 2011). To investigate whether the vHip projects into the VMH, we infused into the VMH of 4- to 5-week-old mice with a retrograde tracer, red retrobeads. Four weeks after the dye was injected into the VMH, these mice received footshocks and 90 min later were sacrificed for immunofluorescence (Figure 1A). Figure 1B shows that red fluorescent signals were detected in the vHip and in the prefrontal cortex (PFC). The number of retrobead-positive cells was the same in the vHip and the PFC ($t_{(4)} = 1.569$, $p = 0.19$, unpaired t test) (Figure 1C), indicating that the vHip and the PFC project their outputs to the VMH. However, c-Fos expression (a marker of neuronal activation) was found to be highly co-localized with retrobead-positive cells in the vHip but not in the PFC ($t_{(4)} = 9.464$, $p < 0.001$, unpaired t test) (Figure 1D), indicating that the vHip neurons that were projected into the VMH are more likely to be

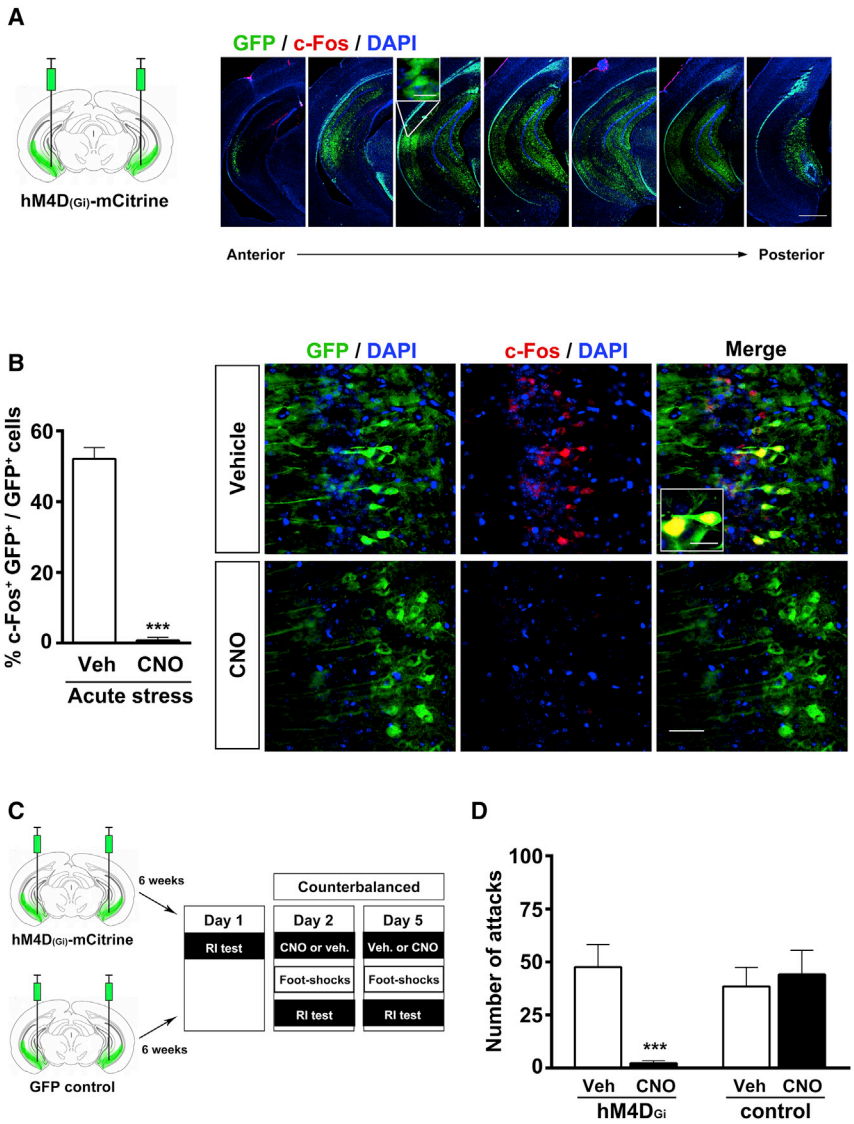

Figure 2. Chemogenetic Inhibition of vHip Activity Reduces Levels of Attack Behavior

(A) Schematic representation of the viral injection sites (AAV5-hSyn-HA-hM4D$_{(Gi)}$-IRES-mCitrine) and images showing the expression of hM4D$_{(Gi)}$-mCitrine in the vHip along the anterior-posterior axis. Scale bar represents 400 μm; inset, scale bar represents 20 μm.

(B) Percentages of c-Fos (red) and GFP (green) double-labeled neurons in the vHip in vehicle-injected (top) and CNO-injected (bottom) mice. The c-Fos expression induced by footshocks in the vHip was significantly decreased by CNO injection (unpaired t test, $t_{(24)} = 15.49$, ***$p < 0.001$; n = 13 brain sections from n = 4 mice /group). Scale bar represents 50 μm; inset, scale bar represents 20 μm.

(C) Schematic experimental procedure. Either CNO (1 mg/kg) or vehicle (Veh) was administrated in hM4D$_{(Gi)}$-expressing and control mice in a counterbalanced manner before footshocks.

(D) CNO treatment reduced the number of attacks in hM4D$_{(Gi)}$-expressing mice but not in control mice (two-way mixed ANOVA drug × transduction interaction, $F_{(1,10)} = 24.55$, $p = 0.0006$; Bonferroni's post hoc test, ***$p < 0.001$ in hM4D$_{(Gi)}$-expressing mice and $p = 0.91$ in control mice). n = 6/group.

Data are represented as mean ± SEM.

activated under acute stress. These results are consistent with the notion that the vHip is linked to the VMH, as previously described (Chiba, 2000; Strange et al., 2014).

Chemogenetic Inhibition of the vHip Blunts Stress-Provoked Attack Behavior

As acute stress selectively activates the VMH-projecting vHip neurons, we hypothesize that vHip activation will contribute to stress-provoked aggression. The engineered human M4 muscarinic receptor (hM4D$_{(Gi)}$) couples to Gi protein and is activated only by clozapine-*N*-oxide (CNO), resulting in neuronal inhibition (Rogan and Roth, 2011). To functionally validate the hM4D$_{(Gi)}$ activity, we bilaterally infused adeno-associated viruses (AAVs) carrying hM4D$_{(Gi)}$ fused to a mCitrine fluorescent protein (AAV5-hSyn-HA-hM4D$_{(Gi)}$-IRES-mCitrine) into the vHip of SI mice. Four weeks later, hM4D$_{(Gi)}$-expressing mice were injected intraperitoneally with 1 mg/kg CNO or vehicle before receiving footshocks. Ninety min later, these mice were sacrificed and the immunofluorescence confirmed that mCitrine was expressed in the vHip (Figure 2A). As shown in Figure 2B, in vehicle-injected mice, footshocks induced c-Fos expression in the hM4D$_{(Gi)}$-expressing vHip neurons. In contrast, c-Fos expression was markedly decreased by a CNO injection ($t_{(24)} = 15.49$, $p < 0.001$), indicating hM4D$_{(Gi)}$ DREADD can effectively inhibit neural activity *in vivo*. We then used the resident-intruder (RI) test to observe the attack behavior of experimental mice. In this test, intruder BALB/c mice with smaller body weight were placed into the home cage of the experimental mice. A separate group of hM4D$_{(Gi)}$-expressing or control (AAV5-hSyn-EGFP) SI mice received CNO or vehicle injection in a counterbalanced manner by using a within-subject design. After vehicle or CNO treatment, these mice received footshocks and then were given the RI test (Figure 2C). Control SI mice dramatically attacked the intruder mice following acute stress (Figure 2D), as seen in our previous studies (Chang et al., 2015). However, we found that CNO treatment reduced the stress-induced attack behavior in hM4D$_{(Gi)}$-expressing mice but not in the control mice (the drug × group interaction, $F_{(1,10)} = 24.55$, $p = 0.0006$ in the two-way mixed-design ANOVA; Bonferroni's post hoc test, $p = 0.0002$ in hM4D$_{(Gi)}$-expressing mice and $p = 0.91$ in control mice)(Figure 2D). The results suggest that the chemogenetic inhibition of vHip neurons blunts stress-provoked attack behavior in the SI mice.

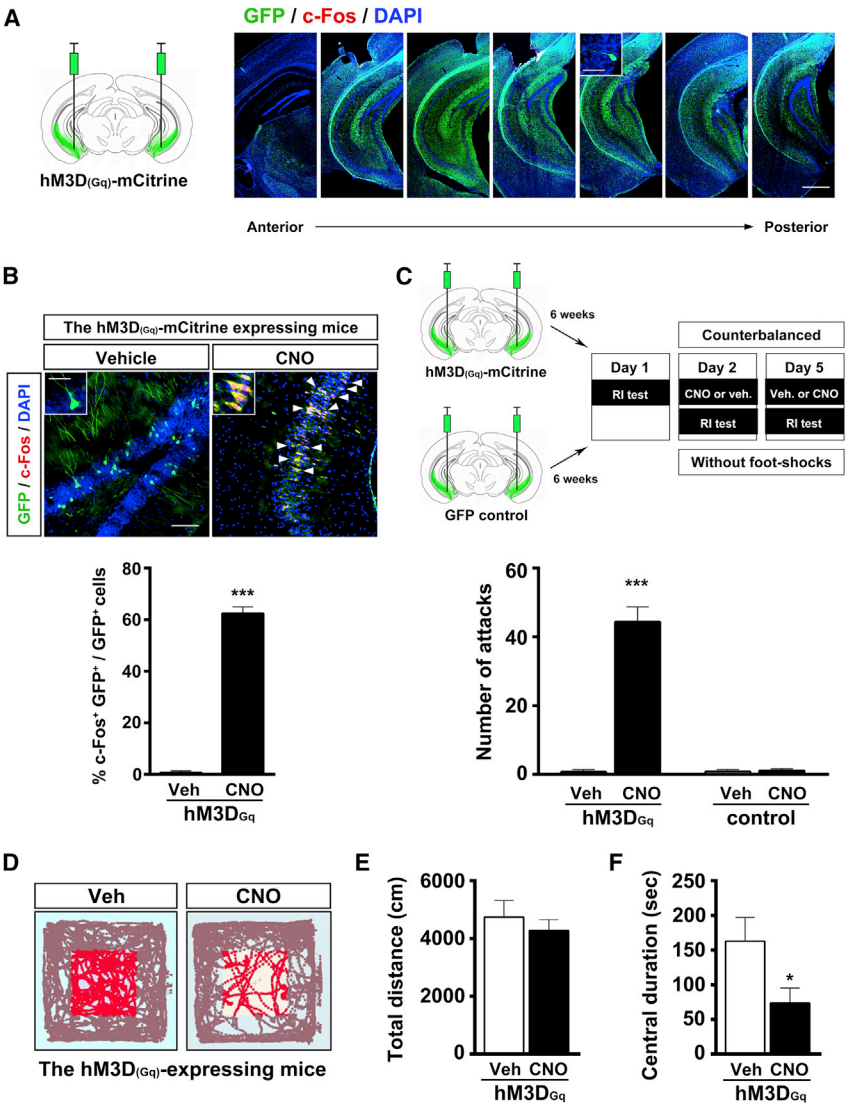

Figure 3. Chemogenetic Activation of vHip Neurons Promotes Attack Behavior

(A) Schematic representation of the viral injection sites (AAV5-hSyn-HA-hM3D$_{(Gq)}$-IRES-mCitrine) and images showing the expression of hM3D$_{(Gq)}$-mCitrine in the vHip along the anterior-posterior axis. Scale bar represents 400 μm; inset, scale bar represents 20 μm.

(B) CNO injection increased c-Fos expression of hM3D$_{(Gq)}$-expressing neurons in the vHip (unpaired t test, t = 24.11, ***p < 0.001; n = 13 brain sections from n = 4 mice/group). Scale bar represents 50 μm; inset, scale bar represents 20 μm.

(C) Schematic illustrating the experimental procedure (top). Either CNO (1 mg/kg) or Veh was injected intraperitoneally into the hM4D$_{(Gq)}$-expressing mice in a counterbalanced manner without footshocks. CNO treatment increased the number of attacks in hM4D$_{(Gi)}$-expressing mice but not in control mice (two-way mixed ANOVA drug × transduction interaction, $F_{(1,9)}$ = 120.1, p < 0.001; Bonferroni's post hoc test, ***p < 0.001 in hM3D$_{(Gq)}$-expressing mice). n = 5 and 6 in hM3D$_{(Gq)}$-expressing and control mice, respectively.

(D–F) The hM3D$_{(Gq)}$-expressing mice performed the open field test after the RI test (n = 5). CNO injection had no effect on the total distance traveled in the open field test in hM3D$_{(Gq)}$-expressing mice (paired t test, $t_{(4)}$ = 1.10, p = 0.33) (E) but significantly decreased time spent in the central zone ($t_{(4)}$ = 3.65, *p = 0.02) (F). Representative tracks in (D).

Data are represented as mean ± SEM.

Chemogenetic vHip Activation Provokes Attack Behavior

To examine whether the vHip activation itself is sufficient to induce attack behavior in the SI mice, we bilaterally infused AAV5-hSyn-HA-hM3D$_{(Gq)}$-IRES-mCitrine or control virus into the vHip of SI mice and activated the vHip neurons by using CNO instead of footshocks. Figure 3A shows the location of the mCitrine expression in the vHip. As shown in Figure 3B, CNO injections significantly increased the c-Fos expression in the hM3D$_{(Gq)}$-expressing vHip neurons compared to vehicle injections ($t_{(24)}$ = 24.11, p < 0.001), indicating that CNO injections induce the activation of hM3D$_{(Gq)}$-expressing neurons. Moreover, without footshocks, the CNO injection alone significantly increased the level of attack behavior in hM3D$_{(Gq)}$-expressing mice but not in control mice (the drug × group interaction, $F_{(1,9)}$ = 120.1, p < 0.0001 in the two-way mixed-design ANOVA; Bonferroni's post hoc test, p < 0.0001 in hM3D$_{(Gq)}$-expressing mice; Figure 3C). Without footshocks, the control mice in neither the vehicle- nor CNO-treatment groups exhibited attack behavior (Figure 3C). The results suggest that the activation of vHip neurons mimicks acute stress effects by promoting attack behavior in SI mice.

In addition, we measured the total distance traveled in the open field test and did not detect any effect of hM3D$_{(Gq)}$ activation on general locomotion (two-tailed paired t test, $t_{(4)}$ = 1.10, p = 0.33; Figures 3D and 3E). However, hM3D$_{(Gq)}$-expressing mice spent less time in the central zone of the open field after a CNO injection (two-tailed paired t test, $t_{(4)}$ = 3.65, p = 0.02; Figure 3F), suggesting the chemogenetic activation of vHip neurons induces anxiety-like behavior. Taken together, the results of the chemogenetic approaches provide converging evidence that hM3D$_{(Gq)}$-activation of vHip neurons promotes attack behavior, whereas the hM4D$_{(Gi)}$-inhibition of vHip neurons blunts footshock-induced attack behavior in the SI mice.

A previous study suggests that under some conditions, AAVs could be neurotoxic and produce unexpected outcomes (van Gestel et al., 2014). To determine whether the AAV transduction itself affects aggressive behavior, we measured the attack behavior 4 weeks after the transduction (day 1 in Figure 2C and Figure 3C) without footshocks or CNO administration. As shown in Figure S1, control virus, hM4D$_{(Gi)}$-IRES-mCitrine, and hM3D$_{(Gq)}$-IRES-mCitrine transduction did not significantly

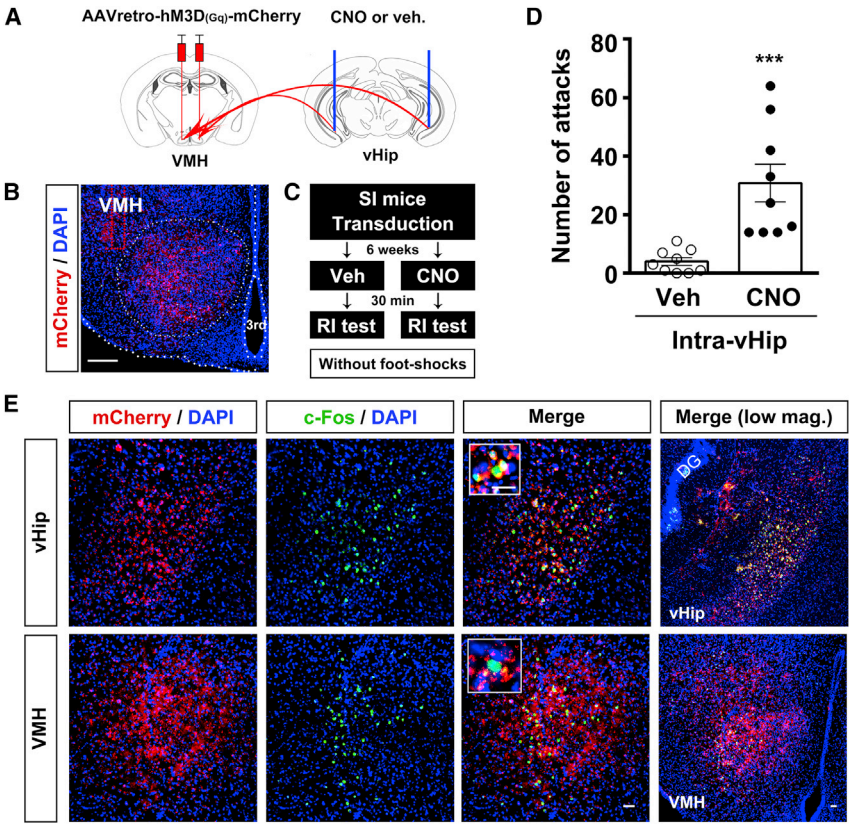

Figure 4. The hM3D$_{(Gq)}$-Mediated Activation of Cell Bodies of vHip Neurons Projecting into the VMH Contributes to Attack Behavior

(A) Schematic representation of the location of AAVrg-hSyn-hM3D$_{(Gq)}$-mCherry transduction in the VMH and the injection of CNO in the vHip.

(B) The representative image of the transduction site of retrograde AAVrg encoding hM3D$_{(Gq)}$-mCherry. 4′,6-Diamidino-2-phenylindole (DAPI) in blue, mCherry in red. Scale bar represents 100 μm.

(C) Schematic illustrating the experimental procedure. CNO (2 μg/μL, 1 μL /side) or Veh was infused into the vHip of the transduced mice without footshocks.

(D) The intra-vHip infusion of CNO-induced attack behavior of mice transducing retrograde AAVrg encoding hM3D$_{(Gq)}$-mCherry into the VMH (unpaired t test, $t = 4.08$, ***$p < 0.001$, n = 9 /group). Data are represented as mean ± SEM.

(E) Representative image of mCherry expression (red) in the vHip (top) indicates that AAVrg encoding hM3D$_{(Gq)}$-mCherry robustly retrogradely projected into the vHip. The intra-vHip infusion of CNO induces c-Fos expression (green) in the hM3D$_{(Gq)}$-expressing vHip neurons (top) and in the VMH (bottom). Scale bar represents 20 μm.

increase attack behavior. Furthermore, there was no difference in attack behavior among the treatments ($F_{(2,14)} = 0.422$, $p = 0.663$), ruling out the non-specific effect of viral transduction.

vHip-VMH Projection Contributes to Stress-Provoked Attack Behavior in SI Mice

It has been shown that AAV-hM4Di DREADDs antegradely trafficked to the axon terminals, and the administration of the DREADDs ligand CNO to the axon terminal area was able to disconnect synaptic communication (Mahler et al., 2014; Stachniak et al., 2014). Next, to examine whether the vHip-VMH pathway contributes to the modulation of aggression, we used this design to selectively silence the nerve terminals projected from the vHip in the VMH. In this test, AAV5-hSyn-hM4D$_{(Gi)}$-mCherry was bilaterally transduced to the vHip, and cannulas were implanted into the VMH of SI mice (Figure S2A). Four weeks later, either CNO or vehicle was infused into the VMH before footshocks. In the counterbalanced within-subjects manner (Figure S2B), the intra-VMH infusion of CNO was more effective at decreasing stress-induced attack behavior than the vehicle infusion ($t_{(4)} = 5.036$, $p < 0.01$; Figure S2C). This result suggests that the neural pathway from the vHip to the VMH is critical in the regulation of acute-stress-provoked attack behavior in SI mice.

To examine the effect of the activation of the vHip cell bodies projecting to the VMH, we next used the retrograde capsid of AAV2, rAAV2-retro, to permit robust retrograde projection and enable sufficiently effective expression to reach the targeted brain areas (Tervo et al., 2016). AAVrg-hSyn-hM3D$_{(Gq)}$-mCherry was bilaterally transduced into the VMH, and cannulas were implanted into the vHip of SI mice (Figures 4A and 4B). Six weeks later, either CNO or vehicle was infused into the vHip in the absence of footshocks (Figure 4C). Figure 4D shows that the bilateral infusion of CNO into the vHip results in more attack behavior than the vehicle infusion ($t_{(16)} = 4.08$, $p < 0.001$). Moreover, the CNO infusion into the vHip induced c-Fos expression in the mCherry-positive vHip neurons (Figure 4E, top), confirming that a CNO infusion activates VMH-projecting vHip neurons. In addition, in the VMH, the mCherry-positive neurons also expressed c-Fos (Figure 4E, bottom), suggesting that the intra-vHip infusion of CNO activated the synapses on VMH neurons. These data suggest that the vHip-VMH pathway is critical in the regulation of attack behavior in SI mice.

vHip Activation Selectively Induces Attack Behavior in Post-Weaning SI Mice but Not in Group-Housed Mice

We next determined whether the activation of vHip neurons provokes attack behavior in GH mice. AAV5-hSyn-hM3D$_{(Gq)}$-mCherry was bilaterally infused into the vHip of age-matched GH mice (Figure 5A). Three to 4 weeks later, these mice were injected with CNO (1 mg/kg) or vehicle, but were not subjected to footshocks. The CNO injection neither induced attack behavior ($t_{(10)} = 0.239$, $p = 0.815$; Figure 5B) nor affected the total distance traveled in the open field test ($t_{(10)} = 1.751$, $p = 0.11$; Figure 5C). However, the CNO-injected mice spent less time in the central zone of the open field ($t_{(10)} = 2.402$, $p < 0.05$; Figure 5D), indicating that the activation of vHip neurons induced anxiety-like behavior in the GH mice. The result is consistent with our previous report that footshocks induce anxiety-like behavior in GH

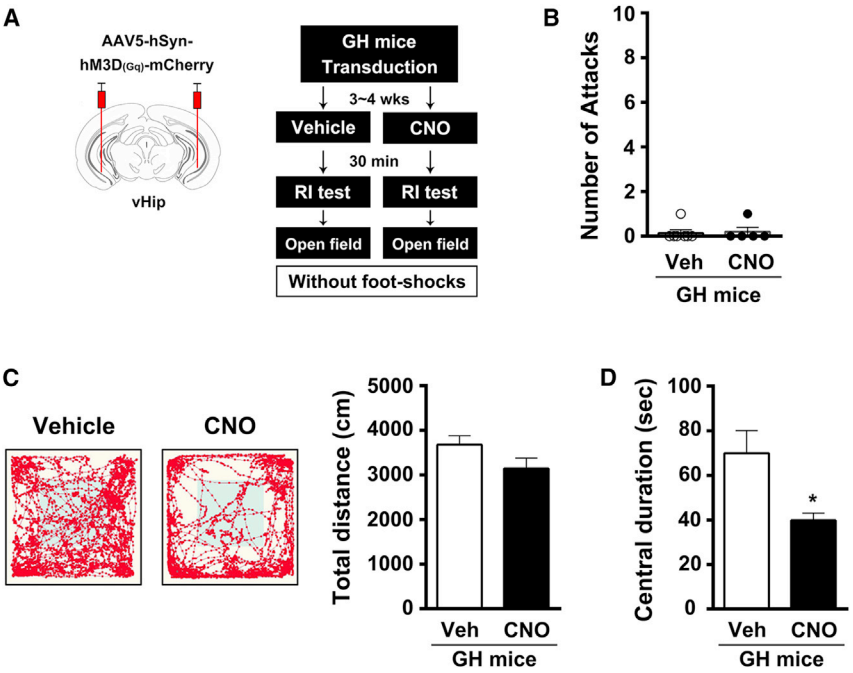

Figure 5. Activation of vHip Neurons Fails to Promote Attack Behavior in Group-Housed Mice

(A) Schematic representation of the viral injection sites (left) and behavioral protocol (right). AAV5-hSyn-hM3D$_{(Gq)}$-mCherry was bilaterally infused into the vHip of the GH mice. Three to 4 weeks later, the mice that did not receive footshocks were injected with either CNO (1 mg/kg) or Veh.

(B) The CNO injection did not affect the number of attacks in the GH mice (unpaired t test, t = 0.24, p = 0.815, n = 7 and 5 in Veh and CNO injection, respectively).

(C and D) CNO-injected GH mice spent less time in the central zone of the open field (D) (unpaired t test, t = 2.40, *p < 0.05). The total distance traveled in the open field test was the same for CNO- and Veh-injected groups (C) (unpaired t test, t = 1.75, p = 0.11). n = 7 and 5 in Veh and CNO injection, respectively. Data are represented as mean ± SEM.

mice (Chang et al., 2015). These results indicate that the vHip activation promotes attack behavior only in SI mice and not in GH mice. In contrast, the vHip activation induces anxiety-like behavior in both SI and GH mice.

Optogenetically Manipulating vHip Glutamatergic Neurons Controls Attack Behavior

Because it is already known that NMDA receptors (NMDA-Rs) are overexpressed in the vHip of SI mice (Chang et al., 2015), we decided to test whether glutamatergic neurons are associated with attack behavior. To determine this, lentiviruses with halorhodopsin (eNpHR3.0) under the control of the CaMKIIα promoter (Yizhar et al., 2011) (LV-CaMKIIα-eNpHR3.0-enhanced yellow fluorescent protein [eYFP]) were transduced into the vHip of SI mice. At the same time, bilateral optical fibers were implanted into the vHip. To verify the eNpHR3.0 function *in vivo*, eNpHR-transduced mice received footshocks and then were divided into two groups. One group of eNpHR-transduced mice received amber light (589 nm, 2 mW for 3 min) through the bilateral implanted optic fibers and the other group did not (Figure 6A). The results show that footshocks increased c-Fos expression in the eNpHR-expressing neurons of the vHip (Figure 6B, top), but the amber light stimulation significantly decreased footshock-induced c-Fos expression (Figure 6B, bottom). Quantification of the results reveals that the number of GFP-positive cells with c-Fos expression decreases significantly more in the light-stimulated group than in the group without light stimulation ($t_{(14)}$ = 26.90, p < 0.001; Figure 6B, right), confirming that the stimulation of eNpHR3.0 by amber light inhibits the activation of vHip glutamatergic neurons.

Following the administration of footshocks, we probed the freely moving mice, which were under optogenetic control in the RI test. These mice were tested in three 3-min time periods, beginning with a light-off (OFF) baseline period, followed by an amber light-on (ON) illumination period, and then a second OFF period (Figure 6C). During this testing, the SI mice attacked and bit the intruders after receiving footshocks. However, the optogenetic inhibition of eNpHR-expressing neurons blunted footshock-provoked attack behavior in a reversible manner (a repeated one-way ANOVA was performed, F = 14.33, p = 0.003, n = 5; Figure 6D; see Videos S1, S2, and S3), suggesting that the optogenetic inhibition of vHip glutamatergic neurons reduces stress-provoked attack behavior.

To examine whether the activation of vHip glutamatergic neurons through light stimulation mimicks stress effects in promoting attack behavior, we expressed a channelrhodopsin-2 (ChR2)-eYFP fusion protein in the vHip glutamatergic neurons by using lentiviruses (LV-CaMKIIα-hChR2(H134R)-eYFP), and bilateral optic fibers were implanted into the vHip of SI mice (Figure 7A). Instead of receiving footshocks, these mice were given blue light stimulation (473 nm, 4 mW in 20 Hz, 5-ms pulse duration for 10 min) before the RI tests. Figure 7B shows that the blue light stimulation induced c-Fos expression in the ChR2-expressing neurons. Quantification of the results reveals that the number of GFP-positive cells with c-Fos expression increased significantly more in the light stimulated group than in the group without light stimulation ($t_{(12)}$ = 21.18, p < 0.001; Figure 7B, right), confirming that photostimulation activates ChR2-expressing vHip glutamatergic neurons. Moreover, the optogenetic activation of vHip glutamatergic neurons induced attack behavior in the ChR2-expressing mice. In contrast, the blue light stimulation in eNpHR-expressing mice had no effect on attack behavior (the blue light × group interaction effect, $F_{(1,7)}$ = 19.58, p = 0.0031 in the two-way mixed-design ANOVA; Bonferroni's post hoc test, p = 0.0016 in ChR2-expressing mice; Figure 7C). These results suggest that the activation of vHip glutamatergic neurons promotes attack behavior. To examine whether the blue light stimulation affected the mice's activity, we also gave the mice an open field test after light illumination. The ChR2- and

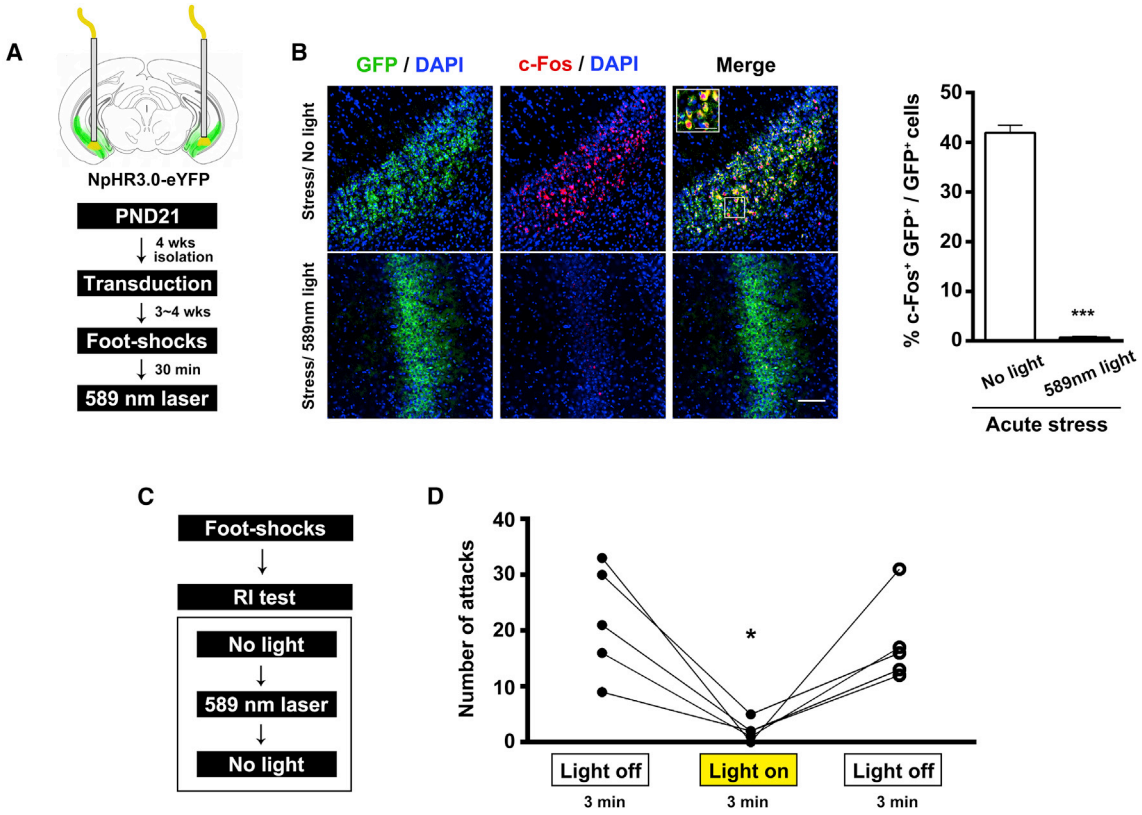

Figure 6. Optogenetic Inhibition of Glutamatergic Neurons in the vHip Blunts Footshock-Provoked Attack Behavior

(A) Schematic representation of bilateral viral injection sites and optic fiber implants. Lentivirus carrying pLenti-CaMKIIα-eNpHR3.0-eYFP was infused into the vHip of SI mice. After 4 weeks of rest in an isolated cage, these mice received footshocks to induce c-Fos expression and then the amber light (589 nm) was delivered through implanted optic fibers.

(B) The optogenetic inhibition of eNpHR-expressing neurons blocked footshock-induced c-Fos expression in the vHip. After footshocks, c-Fos was induced in eNpHR-expressing neurons without amber light delivery (top). Amber light illumination of the vHip *in vivo* reduced c-Fos expression (bottom) (unpaired t test, $t = 26.90$, ***$p < 0.001$). n = 8 brain sections from 3 mice per group. GFP in green, c-Fos in red, DAPI in blue. Scale bar represents 50 μm; inset, scale bar represents 20 μm.

(C) Schematic diagram illustrating the experimental procedure of amber light delivery in three periods of 3 min duration in the RI test.

(D) Optic inhibition of eNpHR-expressing neurons blunted footshock-provoked attack behavior. After footshocks, SI mice exhibited attack behavior. The number of attacks was reduced during the amber light delivery period. Repeated one-way ANOVA, F = 14.33, **p = 0.003; Bonferroni's post hoc test, *$p < 0.05$; ON versus OFF sections, n = 5.

Data are represented as mean ± SEM.

eNpHR-expressing mice traveled the same total distance (two-tailed unpaired t test, $t_{(7)} = 0.068$, p = 0.95; Figure 7D), suggesting that the blue light stimulation does not affect the general activity of mice. However, ChR2-expressing mice spent significantly less time in the central zone than the eNpHR-expressing mice (two-tailed unpaired t test, $t_{(7)} = 3.90$, p = 0.006; Figure 7E), suggesting the optogenetic activation of vHip glutamatergic neurons induces anxiety-like behavior. Taken together, these results suggest that the ChR2-mediated vHip activation induces attack behavior, whereas eNpHR-mediated inhibition of vHip neurons decreases stress-induced attack behavior in SI mice.

DISCUSSION

Accumulating data shed more and more light on the neural activity in the VMH regarding the expression of attack behavior (Hashikawa et al., 2017; Lin et al., 2011), but until now, little was known about its afferent projections that specifically regulate stress-provoked attack behavior. In the present experiments, we used post-weaning SI mice to model abnormal reactive-impulsive aggression in humans because these mice exhibit stress-induced outburst of attack behavior. We found that acute stress (footshocks) induces a selective activation of the vHip neurons projecting into the VMH but without activating the PFC projecting to the VMH. Thus, we first examined whether the vHip activity itself modulates aggression, after which we closely studied the vHip-to-VMH pathway. Using chemogenetic techniques to functionally manipulate neural activity, we have demonstrated that vHip activity is required for stress-provoked attack behavior that can be blunted by the inhibition of vHip neurons. Conversely, the activation of vHip neurons mimics stress effects in promoting attack behavior. To further test whether

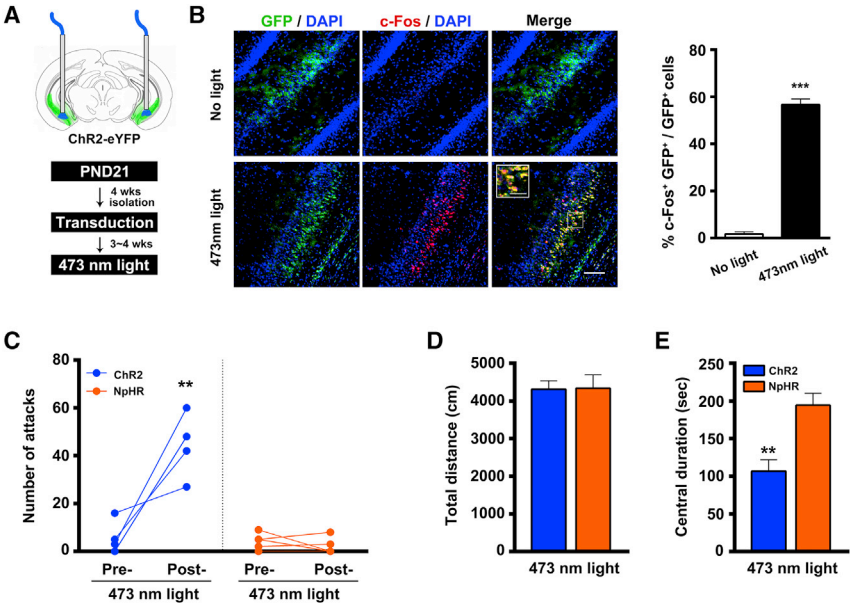

Figure 7. Optogenetic Activation of Glutamatergic Neurons in the vHip Elicits Attack Behavior

(A) Schematic diagram indicating the viral injection site and optic fiber location in the vHip. Lentivirus carrying CaMKIIα-ChR2-eYFP was infused into the vHip. After 3–4 weeks of resting, blue light (473 nm) was delivered by bilateral optic fibers implanted into the vHip.

(B) Blue light illumination of the vHip *in vivo* induced c-Fos expression in the ChR2-expressing neurons (unpaired t test, $t = 21.18$, ***$p < 0.001$). n = 7 brain sections from 3 mice per group. GFP in green, c-Fos in red, DAPI in blue. Scale bar represents 50 μm; inset, scale bar represents 20 μm.

(C) Blue light stimulation significantly increased the number of attacks in ChR2-expressing mice but not in eNpHR-expressing mice. The light × group interaction effect, $F_{(1,7)} = 19.58$, **$p = 0.0031$ in two-way mixed ANOVA; Bonferroni's post hoc test, **$p = 0.0016$ in ChR2-expressing mice; n = 4 and 5 in ChR2- and NpHR-expressing mice, respectively.

(D) The total distance traveled in the open field test was the same for ChR2- and eNpHR-expressing mice after blue light stimulation (unpaired t test, $t = 0.068$, $p = 0.95$).

(E) ChR2-expressing mice spent significantly less time in the central zone than the eNpHR-expressing mice after blue light stimulation (unpaired t test, $t = 3.90$, **$p = 0.006$).

Data are represented as mean ± SEM.

the vHip-VMH projection contributes to the attack behavior, we infused the rAAV2-retro, whose capsid permits retrograde travel to projection neurons, into the VMH. Consistent with the results in the experiments of vHip activation, activating the cell bodies of the vHip neurons projecting into the VMH induced attack behavior. Moreover, to identify the specific cell types involved, we used lentivirus under the control of a CaMKIIα promoter to express eNpHR3.0 into the vHip glutamatergic neurons and found that optogenetic inhibition of eNpHR3.0-expressing glutamatergic neurons blunts footshock-provoked attack behavior. Conversely, optogenetic activation of vHip glutamatergic neurons mimics the effects of acute stress in promoting attack behavior. This is direct evidence showing that the vHip modulates attack behavior through the VMH in SI mice.

Acute stress is a major factor in both human and animal reactive aggression (Kruk et al., 2004; Verona and Kilmer, 2007; Verona et al., 2009). Rhesus monkeys with self-injurious behaviors become more aggressive when their cortisol levels are elevated (Lutz et al., 2003). Rats with respiratory allergies display increased aggressive behavior after acute stress (Tonelli et al., 2008). These studies show that acute stress promotes aggression in subjects with chronic aversive conditions. It is consistent with our model, in which acute stress evoked outbursts of attack behavior in SI mice. In this research we show that under conditions without acute stress (footshocks), the $hM3D_{(Gq)}$-mediated vHip activation induces attack behavior in SI mice (Figure 3) but not in GH mice (Figure 5), suggesting that vHip activation is a promoting factor but not a trigger factor for the expression of attack behavior. There are several possibilities that vHip activation induced attack behavior in the SI mice but not in the GH mice. First, post-weaning SI induces the abnormal development of the brain (Fone and Porkess, 2008) and abnormal phenotypes, such as a deficient prepulse inhibition (PPI) of the acoustic startle reflex, depression-like behavior, and the overexpression of NMDA receptors in the vHip (Chang et al., 2015). It has been reported that NMDA-induced excitotoxic lesions in the vHip disrupt sensorimotor gating, as measured by the PPI of startle (Miller et al., 2010; Shoemaker et al., 2005; Swerdlow et al., 2004). Deficient PPI might promote the susceptibility in SI mice to acute stress and decrease the threshold of their expression of aggression. Thus, it is possible that the SI mice with deficient PPI exhibited an impairment in their ability to integrate external environmental cues and resorted to aggression as a response to certain situations. Second, it has been reported that there is a fast mutual positive feedback between the adrenocortical stress response and aggression induced by stimulation in the hypothalamic aggressive area. Corticosterone injections facilitate hypothalamic attacks, which, in turn, rapidly activate the adrenocortical response (Kruk et al., 2004), implying that the dysregulation of the hypothalamic-pituitary-adrenal (HPA) axis may contribute to escalation of stress-related aggression. Importantly, the hippocampus is a key brain area that controls the function of the HPA axis. Given that early-life stress-induced hippocampal malfunctions dysregulates the HPA axis (Sánchez et al., 2001), the threshold for attack behavior could decrease in the SI mice. In line with this view, we previously found that SI mice exhibited vHip hyperactivation due to the enhanced expression of NMDA receptors (Chang et al., 2015). In the present study, the ChR2-mediated activation of glutamatergic vHip

neurons induced attack behavior even without acute stress, apparently mimicking the acute stress effect on aggression in the SI mice. Moreover, both NpHR3.0-mediated and $hM4D_{(Gi)}$-mediated vHip inhibition blocked the stress-induced outburst of attack behavior. Additionally, acute stress did not induce attack behavior in the GH mice (Chang et al., 2015; Chang et al., 2018). Based on these observations, it seems logical to conclude that SI mice exhibit a decreased threshold for attack behavior. Future studies should examine the synaptic mechanism of the VMH neurons that trigger attack behavior in SI mice and try to determine whether the vHip dysfunction is responsible for its changes. Third, post-weaning SI has been shown to induce serotonin hypofunction in the hippocampus (Veenema, 2009). It should be noted that the bulk of evidence indicates that a serotonergic deficiency contributes to impulsive aggression and violence (Bortolato et al., 2013; Manchia et al., 2017). Mice with null mutants of tryptophan hydroxylase-2 (Tph2), a key enzyme of serotonin biosynthesis in the brain, display strong aggressiveness (Mosienko et al., 2012) as well as alterations in their HPA axis (Gutknecht et al., 2015). Moreover, there are reports that specific subtypes of serotonergic neurons can modulate aggressive behavior (Niederkofler et al., 2016) and serotonergic innervation is markedly dense in the vHip (Sahay and Hen, 2007). Future studies should examine serotonergic functions in vHip neurons projecting to the VMH in the post-weaning socially isolated mice.

The hippocampus is a functionally heterogeneous structure along its longitudinal axis; the dorsal hippocampus is involved in learning and spatial memory, whereas the vHip regulates emotions, such as anxiety, approach-avoidance conflict, and motivated behaviors (Bannerman et al., 2014; Fanselow and Dong, 2010; Fone and Porkess, 2008; Kheirbek et al., 2013; Schumacher et al., 2016). It has been reported that the dorsal CA1 of hippocampus is enriched in place cells and the ventral CA1 is enriched in anxiety cells (Jimenez et al., 2018). Moreover, rats with selectively removed vHip exhibit less anxiety and fear in behavioral tests and have lower plasma corticosterone concentrations when kept in a restricted bright chamber (Bannerman et al., 2003; Kjelstrup et al., 2002). Complete hippocampus lesions, particularly vHip lesions, significantly reduce defensive behavior provoked by footshocks (Blanchard et al., 2005; Pentkowski et al., 2006). Recent studies have shown that the activation of vHip itself or its outputs to the mPFC, the BLA, and lateral hypothalamus enhanced anxiety-like behaviors (Adhikari et al., 2010; Felix-Ortiz et al., 2013; Jimenez et al., 2018; Padilla-Coreano et al., 2016; Parfitt et al., 2017). Consistent with these studies, we have found that vHip activation induced anxiety-like behavior in both SI and GH mice. However, the vHip activation does not induce attack behavior in GH mice, suggesting that increased anxiety alone was not sufficient to induce aggression.

In summary, our results reveal a previously unappreciated role of the vHip-VMH neural circuitry in attack behavior, which occurs under stressful conditions in post-weaning socially isolated mice. As impulsive aggression presents a serious social problem, understanding how stress provokes aggression makes a valuable contribution for the development of therapeutic strategies in controlling inappropriate impulsive behavior.

STAR★METHODS

Detailed methods are provided in the online version of this paper and include the following:

- KEY RESOURCES TABLE
- LEAD CONTACT AND MATERIALS AVAILABILITY
- EXPERIMENTAL MODEL AND SUBJECT DETAILS
  - Experimental Models
  - Subject Details
- METHOD DETAILS
  - Lentivirus production
  - Laser delivery
  - Chemicals
  - Behavioral tests
  - Immunofluorescence
- QUANTIFICATION AND STATISTICAL ANALYSIS

SUPPLEMENTAL INFORMATION

Supplemental Information can be found online at https://doi.org/10.1016/j.celrep.2019.07.005.

ACKNOWLEDGMENTS

We thank Dr. Chun-Lin Su for critical reading of the manuscript. We thank Dr. Bryan Roth for gifts of chemogenetic plasmids and thank Dr. Karl Deisseroth for gifts of optogenetic plasmids. We thank Dr. Allen Walzem for proofreading the manuscript. The National Health Research Institute (NHRI-EX104-10117NI and NHRI-EX107-10730NI) and the Ministry of Science and Technology, Taiwan (MOST 104-2320-B-006-009-MY3, MOST 107-2320-B-006-047, and MOST 107-2811-B-006-011) supported this work.

AUTHOR CONTRIBUTIONS

C.-H.C. performed the experiments and analyzed the data. P.-W.G. supervised the project. C.-H.C. and P.-W.G. designed the study and wrote the manuscript.

DECLARATION OF INTERESTS

The authors declare they have no competing interests.

Received: December 24, 2018
Revised: May 29, 2019
Accepted: June 27, 2019
Published: July 30, 2019

REFERENCES

Adamec, R.E. (1991). Partial kindling of the ventral hippocampus: identification of changes in limbic physiology which accompany changes in feline aggression and defense. Physiol. Behav. *49*, 443–453.

Adamec, R.E., and Stark-Adamec, C. (1983). Partial kindling and emotional bias in the cat: lasting aftereffects of partial kindling of the ventral hippocampus. II. Physiological changes. Behav. Neural Biol. *38*, 223–239.

Adhikari, A., Topiwala, M.A., and Gordon, J.A. (2010). Synchronized activity between the ventral hippocampus and the medial prefrontal cortex during anxiety. Neuron *65*, 257–269.

Anderson, D.J. (2012). Optogenetics, sex, and violence in the brain: implications for psychiatry. Biol. Psychiatry *71*, 1081–1089.

Bannerman, D.M., Grubb, M., Deacon, R.M., Yee, B.K., Feldon, J., and Rawlins, J.N. (2003). Ventral hippocampal lesions affect anxiety but not spatial learning. Behav. Brain Res. *139*, 197–213.

Bannerman, D.M., Sprengel, R., Sanderson, D.J., McHugh, S.B., Rawlins, J.N., Monyer, H., and Seeburg, P.H. (2014). Hippocampal synaptic plasticity, spatial memory and anxiety. Nat. Rev. Neurosci. *15*, 181–192.

Blanchard, D.C., Canteras, N.S., Markham, C.M., Pentkowski, N.S., and Blanchard, R.J. (2005). Lesions of structures showing FOS expression to cat presentation: effects on responsivity to a Cat, Cat odor, and nonpredator threat. Neurosci. Biobehav. Rev. *29*, 1243–1253.

Bortolato, M., Pivac, N., Muck Seler, D., Nikolac Perkovic, M., Pessia, M., and Di Giovanni, G. (2013). The role of the serotonergic system at the interface of aggression and suicide. Neuroscience *236*, 160–185.

Chang, C.H., Hsiao, Y.H., Chen, Y.W., Yu, Y.J., and Gean, P.W. (2015). Social isolation-induced increase in NMDA receptors in the hippocampus exacerbates emotional dysregulation in mice. Hippocampus *25*, 474–485.

Chang, C.H., Su, C.L., and Gean, P.W. (2018). Mechanism underlying NMDA blockade-induced inhibition of aggression in post-weaning socially isolated mice. Neuropharmacology *143*, 95–105.

Chiba, T. (2000). Collateral projection from the amygdalo–hippocampal transition area and CA1 to the hypothalamus and medial prefrontal cortex in the rat. Neurosci. Res. *38*, 373–383.

Dorfman, H.M., Meyer-Lindenberg, A., and Buckholtz, J.W. (2014). Neurobiological mechanisms for impulsive-aggression: the role of MAOA. Curr. Top. Behav. Neurosci. *17*, 297–313.

Fanselow, M.S., and Dong, H.W. (2010). Are the dorsal and ventral hippocampus functionally distinct structures? Neuron *65*, 7–19.

Felix-Ortiz, A.C., Beyeler, A., Seo, C., Leppla, C.A., Wildes, C.P., and Tye, K.M. (2013). BLA to vHPC inputs modulate anxiety-related behaviors. Neuron *79*, 658–664.

Fone, K.C., and Porkess, M.V. (2008). Behavioural and neurochemical effects of post-weaning social isolation in rodents-relevance to developmental neuropsychiatric disorders. Neurosci. Biobehav. Rev. *32*, 1087–1102.

Gutknecht, L., Popp, S., Waider, J., Sommerlandt, F.M., Göppner, C., Post, A., Reif, A., van den Hove, D., Strekalova, T., Schmitt, A., et al. (2015). Interaction of brain 5-HT synthesis deficiency, chronic stress and sex differentially impact emotional behavior in Tph2 knockout mice. Psychopharmacology (Berl.) *232*, 2429–2441.

Hashikawa, K., Hashikawa, Y., Tremblay, R., Zhang, J., Feng, J.E., Sabol, A., Piper, W.T., Lee, H., Rudy, B., and Lin, D. (2017). Esr1^{+} cells in the ventromedial hypothalamus control female aggression. Nat. Neurosci. *20*, 1580–1590.

Jimenez, J.C., Su, K., Goldberg, A.R., Luna, V.M., Biane, J.S., Ordek, G., Zhou, P., Ong, S.K., Wright, M.A., Zweifel, L., et al. (2018). Anxiety Cells in a Hippocampal-Hypothalamic Circuit. Neuron *97*, 670–683.e6.

Kheirbek, M.A., Drew, L.J., Burghardt, N.S., Costantini, D.O., Tannenholz, L., Ahmari, S.E., Zeng, H., Fenton, A.A., and Hen, R. (2013). Differential control of learning and anxiety along the dorsoventral axis of the dentate gyrus. Neuron *77*, 955–968.

Kjelstrup, K.G., Tuvnes, F.A., Steffenach, H.A., Murison, R., Moser, E.I., and Moser, M.B. (2002). Reduced fear expression after lesions of the ventral hippocampus. Proc. Natl. Acad. Sci. USA *99*, 10825–10830.

Kruk, M.R., Halász, J., Meelis, W., and Haller, J. (2004). Fast positive feedback between the adrenocortical stress response and a brain mechanism involved in aggressive behavior. Behav. Neurosci. *118*, 1062–1070.

Lee, H., Kim, D.W., Remedios, R., Anthony, T.E., Chang, A., Madisen, L., Zeng, H., and Anderson, D.J. (2014). Scalable control of mounting and attack by Esr1+ neurons in the ventromedial hypothalamus. Nature *509*, 627–632.

Leroy, F., Park, J., Asok, A., Brann, D.H., Meira, T., Boyle, L.M., Buss, E.W., Kandel, E.R., and Siegelbaum, S.A. (2018). A circuit from hippocampal CA2 to lateral septum disinhibits social aggression. Nature *564*, 213–218.

Lin, D., Boyle, M.P., Dollar, P., Lee, H., Lein, E.S., Perona, P., and Anderson, D.J. (2011). Functional identification of an aggression locus in the mouse hypothalamus. Nature *470*, 221–226.

Lutz, C., Marinus, L., Chase, W., Meyer, J., and Novak, M. (2003). Self-injurious behavior in male rhesus macaques does not reflect externally directed aggression. Physiol. Behav. *78*, 33–39.

Maggio, N., and Segal, M. (2012). Steroid modulation of hippocampal plasticity: switching between cognitive and emotional memories. Front. Cell. Neurosci. *6*, 12.

Mahler, S.V., Vazey, E.M., Beckley, J.T., Keistler, C.R., McGlinchey, E.M., Kaufling, J., Wilson, S.P., Deisseroth, K., Woodward, J.J., and Aston-Jones, G. (2014). Designer receptors show role for ventral pallidum input to ventral tegmental area in cocaine seeking. Nat. Neurosci. *17*, 577–585.

Manchia, M., Carpiniello, B., Valtorta, F., and Comai, S. (2017). Serotonin Dysfunction, Aggressive Behavior, and Mental Illness: Exploring the Link Using a Dimensional Approach. ACS Chem. Neurosci. *8*, 961–972.

Miczek, K.A., de Boer, S.F., and Haller, J. (2013). Excessive aggression as model of violence: a critical evaluation of current preclinical methods. Psychopharmacology (Berl.) *226*, 445–458.

Miller, E.J., Saint Marie, L.R., Breier, M.R., and Swerdlow, N.R. (2010). Pathways from the ventral hippocampus and caudal amygdala to forebrain regions that regulate sensorimotor gating in the rat. Neuroscience *165*, 601–611.

Mosienko, V., Bert, B., Beis, D., Matthes, S., Fink, H., Bader, M., and Alenina, N. (2012). Exaggerated aggression and decreased anxiety in mice deficient in brain serotonin. Transl. Psychiatry *2*, e122.

Niederkofler, V., Asher, T.E., Okaty, B.W., Rood, B.D., Narayan, A., Hwa, L.S., Beck, S.G., Miczek, K.A., and Dymecki, S.M. (2016). Identification of Serotonergic Neuronal Modules that Affect Aggressive Behavior. Cell Rep. *17*, 1934–1949.

Padilla-Coreano, N., Bolkan, S.S., Pierce, G.M., Blackman, D.R., Hardin, W.D., Garcia-Garcia, A.L., Spellman, T.J., and Gordon, J.A. (2016). Direct Ventral Hippocampal-Prefrontal Input Is Required for Anxiety-Related Neural Activity and Behavior. Neuron *89*, 857–866.

Parfitt, G.M., Nguyen, R., Bang, J.Y., Aqrabawi, A.J., Tran, M.M., Seo, D.K., Richards, B.A., and Kim, J.C. (2017). Bidirectional Control of Anxiety-Related Behaviors in Mice: Role of Inputs Arising from the Ventral Hippocampus to the Lateral Septum and Medial Prefrontal Cortex. Neuropsychopharmacology *42*, 1715–1728.

Pentkowski, N.S., Blanchard, D.C., Lever, C., Litvin, Y., and Blanchard, R.J. (2006). Effects of lesions to the dorsal and ventral hippocampus on defensive behaviors in rats. Eur. J. Neurosci. *23*, 2185–2196.

Radaelli, D., Poletti, S., Dallaspezia, S., Colombo, C., Smeraldi, E., and Benedetti, F. (2012). Neural responses to emotional stimuli in comorbid borderline personality disorder and bipolar depression. Psychiatry Res. *203*, 61–66.

Rogan, S.C., and Roth, B.L. (2011). Remote control of neuronal signaling. Pharmacol. Rev. *63*, 291–315.

Rossi, R., Lanfredi, M., Pievani, M., Boccardi, M., Beneduce, R., Rillosi, L., Giannakopoulos, P., Thompson, P.M., Rossi, G., and Frisoni, G.B. (2012). Volumetric and topographic differences in hippocampal subdivisions in borderline personality and bipolar disorders. Psychiatry Res. *203*, 132–138.

Ruocco, A.C., Amirthavasagam, S., and Zakzanis, K.K. (2012). Amygdala and hippocampal volume reductions as candidate endophenotypes for borderline personality disorder: a meta-analysis of magnetic resonance imaging studies. Psychiatry Res. *201*, 245–252.

Sahay, A., and Hen, R. (2007). Adult hippocampal neurogenesis in depression. Nat. Neurosci. *10*, 1110–1115.

Sánchez, M.M., Ladd, C.O., and Plotsky, P.M. (2001). Early adverse experience as a developmental risk factor for later psychopathology: evidence from rodent and primate models. Dev. Psychopathol. *13*, 419–449.

Schumacher, A., Vlassov, E., and Ito, R. (2016). The ventral hippocampus, but not the dorsal hippocampus is critical for learned approach-avoidance decision making. Hippocampus *26*, 530–542.

Shoemaker, J.M., Saint Marie, R.L., Bongiovanni, M.J., Neary, A.C., Tochen, L.S., and Swerdlow, N.R. (2005). Prefrontal D1 and ventral hippocampal N-methyl-D-aspartate regulation of startle gating in rats. Neuroscience *135*, 385–394.

Stachniak, T.J., Ghosh, A., and Sternson, S.M. (2014). Chemogenetic synaptic silencing of neural circuits localizes a hypothalamus→midbrain pathway for feeding behavior. Neuron *82*, 797–808.

Strange, B.A., Witter, M.P., Lein, E.S., and Moser, E.I. (2014). Functional organization of the hippocampal longitudinal axis. Nat. Rev. Neurosci. *15*, 655–669.

Swerdlow, N.R., Shoemaker, J.M., Noh, H.R., Ma, L., Gaudet, I., Munson, M., Crain, S., and Auerbach, P.P. (2004). The ventral hippocampal regulation of prepulse inhibition and its disruption by apomorphine in rats are not mediated via the fornix. Neuroscience *123*, 675–685.

Takahashi, A., Nagayasu, K., Nishitani, N., Kaneko, S., and Koide, T. (2014). Control of intermale aggression by medial prefrontal cortex activation in the mouse. PLoS One *9*, e94657.

Tervo, D.G., Hwang, B.Y., Viswanathan, S., Gaj, T., Lavzin, M., Ritola, K.D., Lindo, S., Michael, S., Kuleshova, E., Ojala, D., et al. (2016). A Designer AAV Variant Permits Efficient Retrograde Access to Projection Neurons. Neuron *92*, 372–382.

Tonelli, L.H., Hoshino, A., Katz, M., and Postolache, T.T. (2008). Acute Stress Promotes Aggressive-Like Behavior in Rats Made Allergic to Tree Pollen. Int. J. Child Health Hum. Dev. *1*, 305–312.

Toth, M., Fuzesi, T., Halasz, J., Tulogdi, A., and Haller, J. (2010). Neural inputs of the hypothalamic "aggression area" in the rat. Behav. Brain Res. *215*, 7–20.

Toth, M., Mikics, E., Tulogdi, A., Aliczki, M., and Haller, J. (2011). Post-weaning social isolation induces abnormal forms of aggression in conjunction with increased glucocorticoid and autonomic stress responses. Horm. Behav. *60*, 28–36.

Unger, E.K., Burke, K.J., Jr., Yang, C.F., Bender, K.J., Fuller, P.M., and Shah, N.M. (2015). Medial amygdalar aromatase neurons regulate aggression in both sexes. Cell Rep. *10*, 453–462.

van Gestel, M.A., Boender, A.J., de Vrind, V.A., Garner, K.M., Luijendijk, M.C., and Adan, R.A. (2014). Recombinant adeno-associated virus: efficient transduction of the rat VMH and clearance from blood. PLoS One *9*, e97639.

Veenema, A.H. (2009). Early life stress, the development of aggression and neuroendocrine and neurobiological correlates: what can we learn from animal models? Front. Neuroendocrinol. *30*, 497–518.

Verona, E., and Kilmer, A. (2007). Stress exposure and affective modulation of aggressive behavior in men and women. J. Abnorm. Psychol. *116*, 410–421.

Verona, E., Sadeh, N., and Curtin, J.J. (2009). Stress-induced asymmetric frontal brain activity and aggression risk. J. Abnorm. Psychol. *118*, 131–145.

Wong, L.C., Wang, L., D'Amour, J.A., Yumita, T., Chen, G., Yamaguchi, T., Chang, B.C., Bernstein, H., You, X., Feng, J.E., et al. (2016). Effective Modulation of Male Aggression through Lateral Septum to Medial Hypothalamus Projection. Curr. Biol. *26*, 593–604.

Yang, T., Yang, C.F., Chizari, M.D., Maheswaranathan, N., Burke, K.J., Jr., Borius, M., Inoue, S., Chiang, M.C., Bender, K.J., Ganguli, S., et al. (2017). Social Control of Hypothalamus-Mediated Male Aggression. Neuron *95*, 955–970.

Yizhar, O., Fenno, L.E., Davidson, T.J., Mogri, M., and Deisseroth, K. (2011). Optogenetics in neural systems. Neuron *71*, 9–34.

STAR★METHODS

KEY RESOURCES TABLE

REAGENT or RESOURCE	SOURCE	IDENTIFIER
Antibodies		
Unconjugated AffiniPure Fab fragment goat anti-mouse IgG (H+L)	Jackson ImmunoResearch	Cat # 115-007-003; RRID: AB_2338476
rabbit anti-GFP	Genetex	Cat # GTX113617; RRID: AB_1950371
rabbit anti-mCherry	Genetex	Cat # GTX128508; RRID: AB_2721247
mouse anti-cFos	Genetex	Cat # GTX60996; RRID: AB_2810303
Alexa Fluor 594 Fab fragment goat anti-mouse	Jackson ImmunoResearch	Cat # 115-587-003; RRID: AB_2338900
Alexa Fluor 488 Fab fragment goat anti-mouse	Jackson ImmunoResearch	Cat # 115-547-003; RRID: AB_2338869
Alexa Fluor 488 goat anti-rabbit	Jackson ImmunoResearch	Cat # 111-545-003; RRID: AB_2338046
Alexa Fluor 594 goat anti-rabbit	Jackson ImmunoResearch	Cat # 111-585-003; RRID: AB_2338059
Bacterial and Virus Strains		
AAV5-hSyn-HA-hM3D(Gq)-IRES-mCitrine	the University of North Carolina at Chapel Hill, Gene Therapy Center Vector Core	AV4619B
AAV5-hSyn-HA-hM4D(Gi)-IRES-mCitrine	the University of North Carolina at Chapel Hill, Gene Therapy Center Vector Core	AV4623F
AAV5-hSyn-hM3D(Gq)-mCherry	the University of North Carolina at Chapel Hill, Gene Therapy Center Vector Core	AV6332B
AAV5-hSyn-EGFP	the University of North Carolina at Chapel Hill, Gene Therapy Center Vector Core	AV4657C
AAVrg-hSyn-hM3D(Gq)-mCherry	Addgene	# 50474-AAVrg
AAVrg-hSyn-hM4D(Gi)-mCherry	Addgene	# 50475-AAVrg
Chemicals, Peptides, and Recombinant Proteins		
CAS-Block reagent	Invitrogen	Cat # 008120
DAPI	Sigma-Aldrich	Cat # 32670
Clozapine *N*-oxide	Tocris	Cat # 6329
red retrobeads	Lumafluor Inc.	Red IX RetroBeads
Experimental Models: Organisms/Strains		
C57BL/6JNarl	the National Laboratory Animal Center (Taiwan)	RMRC11005
BALB/cByJNarl	the National Laboratory Animal Center (Taiwan)	RMRC11001
Recombinant DNA		
pLenti-CaMKIIα-hChR2(H134R)-EYFP-WPRE	Addgene	# 20944
pLenti-CaMKIIα-eNpHR3.0-EYFP	Addgene	# 26970
Software and Algorithms		
EthoVison XT8.5 software	Noldus	http://www.noldus.com
GraphPad Prism 6	GraphPad	https://www.graphpad.com
MetaVue	Molecular Devices	https://www.moleculardevices.com
Optogenetics TTL pulse generator	Doric	OTPG4
Other		
Cannula (C315GS-2-SP guide 26GA 38834 2mm ped, cut 5mm below pedestal)	PlasticsOne	Custom made
The microsyringe pump	Kd Scientific	KDS-101

(*Continued on next page*)

Continued

REAGENT or RESOURCE	SOURCE	IDENTIFIER
The 10 μl microsyringe	Hamilton	80330
Implantable optic fibers (length = 4 mm, 200 μm core, NA = 0.39) with ceramic stick ferrules	Thorlabs	Custom made
The 473 nm DPSS laser	Changchun New Industries Optoelectronics Technology (CNI)	MBL-III-473-100mW
The 589 nm DPSS laser	Changchun New Industries Optoelectronics Technology (CNI)	MGL-589-100mW
MM Simplex 62.5um / 900um Patch Cord	Precision Fiber Products	MMSBT62-2-M02-2
The MM 62.5 μm 1x2 coupler, 850/1310 dual window, 50/50 split ratio, 900 μm fiber	Precision Fiber Products	CPL128513-50-6-9-150-1000-2-8
The fiber-optic 1x1 rotary joint	Doric	FRJ_1x1_FC-FC

LEAD CONTACT AND MATERIALS AVAILABILITY

Further information and requests for resources and reagents should be directed to the Lead Contact, Po-Wu Gean (powu@mail.ncku.edu.tw).

EXPERIMENTAL MODEL AND SUBJECT DETAILS

Experimental Models

The male C57BL/6JNarl mice were purchased 21∼28 days after birth from the National Laboratory Animal Center (Taiwan) and were randomly divided into the group-housing (five mice per cage) and the socially isolated (one mice per cage) groups. All mice were given free access to water and food on a 12h /12h light/dark cycle. The socially isolated (SI) mice were not handled more than once a week. All experiments were approved by the Institutional Animal Care and Use Committee of the National Cheng Kung University (NCKU).

Subject Details

Stereotaxic injection

For experiments with retrogradely traveling tracers, 7∼8 week-old SI mice were anesthetized with sodium pentobarbital (50mg/kg) and mounted on a stereotaxic apparatus (Kopf, USA). To identify which brain areas project into the VMH, red retrobeads (about 0.1 μL per side; Red IX RetroBeads, Lumafluor Inc., USA) were bilaterally infused into the VMH (anterioposterior, −1.5 mm; mediolateral, ± 0.6 mm; dorsoventral, −5.5 mm) through 28 GA stainless steel tubes at a rate of 0.1 μl/min using a microsyringe pump (KDS-101, Kd Scientific, USA). After completion of the infusion, the tube was left for an additional 10 min and then slowly withdrawn. Four weeks after retrobead injections, immunofluorescence studies were performed on the mice, as described below. In the chemogenetic experiments, the AAV5-hSyn-HA-hM3D$_{(Gq)}$-IRES-mCitrine, AAV5-hSyn-hM3D$_{(Gq)}$-mCherry, AAV5-hSyn-HA-hM4D$_{(Gi)}$-IRES-mCitrine, or AAV5-hSyn-EGFP were bilaterally infused into the vHip (anterioposterior, −3.2 mm; mediolateral, ± 3.2 mm; dorsoventral, −4.0 mm) by a 10 μL microsyringe (80330, Hamilton, USA) at a rate of 0.1 μl/min. In the retrograde chemogenetic experiments, the AAVrg-hSyn-hM3D$_{(Gq)}$-mCherry (#50474-AAVrg) and AAVrg-hSyn-hM4D$_{(Gi)}$-mCherry (#50475-AAVrg) were infused into the VMH (anterioposterior, −1.5 mm; mediolateral, ± 0.6 mm; dorsoventral, −5.5 mm) and, at the same time, cannulas (C315GS-2-SP guide 26GA 38834 2mm ped, cut 5mm below pedestal) were implanted into the vHip. For optogenetic experiments, the Lenti-CaMKIIα-hChR2(H134R)-EYFP-WPRE and Lenti-CaMKIIα-eNpHR3.0-EYFP were infused into the vHip and, at the same time, bilateral implantable optic fibers (length = 4 mm, 200 μm core, NA = 0.39; Thorlabs, USA) with ceramic stick ferrules (Precision Fiber Products, USA) were implanted into the vHip. Implantable fibers were adhered to the skull with Loctite 454 Prism surface insensitive gel (Loctite, USA). Mice were given a recovery period for 3-4 weeks before behavioral tests were administered.

METHOD DETAILS

Lentivirus production

To generate lentivirus carrying target vectors, the target plasmids [pLenti-CaMKIIα-hChR2(H134R)-EYFP-WPRE (Addgene #20944) or pLenti-CaMKIIα-eNpHR3.0-EYFP (Addgene #26970)] and pCMV-dR8.91 and pMD2.G plasmids (Institute of Molecular Biology, Academia Sinica, Taiwan) were co-transduced into HEK293T cells using Lipofectamine LTX with Plus™ Reagent (Invitrogen, USA) according to the manufacturer's instructions.

Laser delivery

For optical stimulation, a 473 nm (MBL-III-473-100mW, CNI, China) or 589 nm DPSS laser (MGL-589-100mW, CNI, China) was connected to a patch cord with a pair of FC/PC connectors (Precision Fiber Products, USA). The fiber-optic 1x1 rotary joint (Doric, Canada) connected this patch cord and a MM 62.5 μm 1x2 coupler, 850/1310 dual window, 50/50 split ratio, 900 μm fiber (Precision Fiber Products, USA), which was connected to implantable fibers. The 473 nm laser (blue light) was delivered at 4 mW in 20 Hz, 5 ms light pulses for 10 min. The 589 nm laser (amber light) consisted of constant light at 2 mW for 3 min. All laser output was modulated using an Optogenetics TTL pulse generator (OTPG4, Doric, Canada).

Chemicals

Clozapine-*N*-oxide (CNO) (Enzo Life Science, USA) was dissolved in 0.9% saline. The dose of CNO was 1mg/kg and 2 μg/μl (1 μL /side) for intraperitoneal injection and microinjection, respectively.

Behavioral tests

The open field test to assess anxiety-like behavior in the mice was performed in a square box with a white floor and black walls (40 × 40 × 40 cm) for 10 min. The box was cleaned before each test using 75% ethanol to eliminate the odor of other mice. The total distance that mice traveled in the box was recorded using a Noldus video tracking system and was analyzed with EthoVison XT5.1 software. The resident-intruder (RI) test to assess attack behavior was performed according to previous studies (Chang et al., 2018). Briefly, the SI mice were left in the same cages, but the group-housing mice were individually housed for one night before the RI test. To trigger the stress-induced outburst of aggression, the resident mice were placed on a footshock grid (San Diego Instrument, USA) and received five 0.1 mA, 1sec, foot-shocks with random intervals 30 min before the RI test. An intruder mouse (BALB/c mice with 15 ~18 g of body weight) was then placed into the home cage of the resident mouse for 15 min. Attack behavior aimed toward the intruder is defined as active bites of the resident mice, followed by strong startle responses of the intruder. The behaviors of resident mice were recorded using a SONY digital camera (HDR-XR150, Japan) and scored by trained observers.

Immunofluorescence

Immunostaining studies were performed using c-Fos expression as a marker for neural activity in the ChR2, NpHR3.0, $hM3D_{(Gq)}$, or $hM4D_{(Gi)}$ experiments. Mice were anesthetized with sodium pentobarbital (50 mg/kg) and perfused with 4% paraformaldehyde. The brains were fixed for an additional 24h in ice-cold 4% paraformaldehyde. After incubation with 30% sucrose, brains were sectioned into 40 μm-thick coronal sections using cryostat (CM3050S, Leica). Floating sections were blocked in 0.12mg /ml unconjugated Fab fragment goat anti-mouse IgG (H+L) with CAS-Block agent (Invitrogen, USA) for 2hr at room temperature, followed by rabbit anti-GFP (1:200, Genetex, USA), rabbit anti-mCherry (1:200, Genetex, USA), or mouse anti-cFos (1:200, Genetex, USA) in CAS-Block agent at 4°C overnight. Secondary antibodies with CAS-Block agent (1:200 Alexa Fluor 594 Fab fragment goat anti-mouse, Alexa Fluor 488 Fab fragment goat anti-mouse, Alexa Fluor 488 goat anti-rabbit, or Alexa Fluor 594 goat anti-rabbit, Jackson ImmunoResearch, USA). After rinsing in 0.1% PBST, sections were incubated in 1:1000 DAPI (Sigma, USA) with PBS for 15 min. Images were acquired using a Leica DM2500 Microscope coupled to a digital camera (C10600, HAMAMATSU, Japan). All tests were run in triplicate.

QUANTIFICATION AND STATISTICAL ANALYSIS

Statistical analysis was performed using GraphPad Prism 6 (GraphPad Software, San Diego, CA). Data were expressed as mean ± SEM and were analyzed using either a Student's t test or ANOVA, as indicated. Bonferroni's multiple comparisons test was used as post hoc comparisons of ANOVA. The level of significance was $p < 0.05$.